

Theory of the acoustic realignment of nematic liquid crystals

A. P. Malanoski, V. A. Greanya, B. T. Weslowski, M. S. Spector, J. V. Selinger, and R. Shashidhar*
*Center for Bio/Molecular Science and Engineering, Naval Research Laboratory, Code 6900, 4555 Overlook Avenue SW,
 Washington, DC 20375, USA*

(Received 17 October 2003; published 26 February 2004)

When an ultrasonic wave is applied to a nematic liquid-crystal cell, the molecules change their orientation, leading to a change in the optical intensity transmitted through the cell. Modeling this acousto-optic effect involves three separate theoretical issues: (a) calculating the intensity of sound transmitted through the cell walls into the liquid crystal, (b) determining the consequent realignment of the liquid crystal, and (c) deriving the change in optical transmission through the cell. In this paper, we present a theory that addresses all three of these issues, and thereby reproduces the behavior seen in experiments. The theory shows how the performance depends not only on the liquid-crystal material properties, but also on the geometrical parameters of the system, such as the thickness of the glass walls, thickness of the liquid-crystal layer, angle of the ultrasonic wave, viewing angle, and boundary condition at the glass-liquid crystal interface. The theory predicts that the strong dependence on viewing angle still allows an optical image to be seen for realistic dimensions.

DOI: 10.1103/PhysRevE.69.021705

PACS number(s): 61.30.Gd, 61.30.Dk, 78.20.Hp, 43.35.+d

I. INTRODUCTION

Nematic liquid crystals are well known to exhibit an electro-optic effect, in which an applied electric field realigns the molecules, leading to a change in the optical transmission through the liquid-crystal cell. In addition to the electro-optic effect, nematic liquid crystals also exhibit an acousto-optic effect, in which a low-intensity acoustic-field realigns the molecules, again leading to a change in optical transmission [1–8]. This effect can be exploited to visually observe variations in an acoustic wave that probes the structure of a system. It is already being used in this manner as a means to nondestructively test materials for weaknesses [9–11]. It has further potential applications in medical diagnostics and underwater imaging.

In a previous paper, we proposed a theory for the acousto-optic effect in nematic liquid crystals [12]. This theory agreed with the then available experimental results as a function of the incoming acoustic intensity. However, subsequent experiments by our group investigated the acousto-optic effect as a function of geometric parameters of the cell, particularly the angle of the incoming sound wave, the viewing angle, and the thickness of the liquid-crystal cell [13]. These experiments showed that the acousto-optic effect depends sensitively on all of these geometrical parameters. The dependence on the cell thickness was consistent with the theoretical predictions, but the dependence on the acoustic angle and the viewing angle could not be explained by the theory.

In this paper, we generalize the earlier theory to address the experimental results of Ref. [13]. For this generalization, we note that modeling the acousto-optic effect involves three distinct theoretical issues.

(a) First, we must calculate how much of an incoming sound wave is transmitted through the cell walls into the liquid crystal. We develop a model for the propagation of

sound through the multilayer geometry of water/glass/liquid crystal/glass/water. This model predicts the intensity of the forward- and backward-traveling sound waves within the liquid crystal.

(b) We must then determine how the sound intensity in the liquid-crystal layer interacts with the molecular orientation and realigns the molecules. For this calculation, we use the continuum elastic formalism developed in our earlier paper [12], but extend the theory to higher order in a perturbation series.

(c) Finally, we must derive how the realigned liquid crystal changes the transmission of light through the cell. We present this optics calculation, and show how the results depend on the viewing angle. This angular dependence was not considered in our earlier work, which considered only normal incidence of light.

In the following sections, we present the theoretical work in detail. We compare our results with the experiments in Ref. [13], using appropriate values for the relevant geometric parameters, and find good agreement between theory and experiment. We then use this theoretical approach to simulate the images that would be seen in an acousto-optic device. These calculations show that the viewing-angle dependence allows an optical image to be seen for realistic device dimensions. Thus, the theory shows how an acousto-optic device can be designed for imaging applications.

II. THEORY

As discussed in the introduction, the first problem is to determine the actual sound intensity that reaches the liquid crystal. Figure 1 shows a representation of the system and the sound waves that are present. In order to solve the problem we must assume some form for the sound waves present in each layer. In each layer there are two longitudinal acoustic waves possible, one forward traveling from transmission and one backward traveling from reflection, which we assume travel as plane waves of the form

*Present address: Geo-Centers Inc., Maritime Plaza One, Suite 050, 120 M Street, SE, Washington, DC 20003.

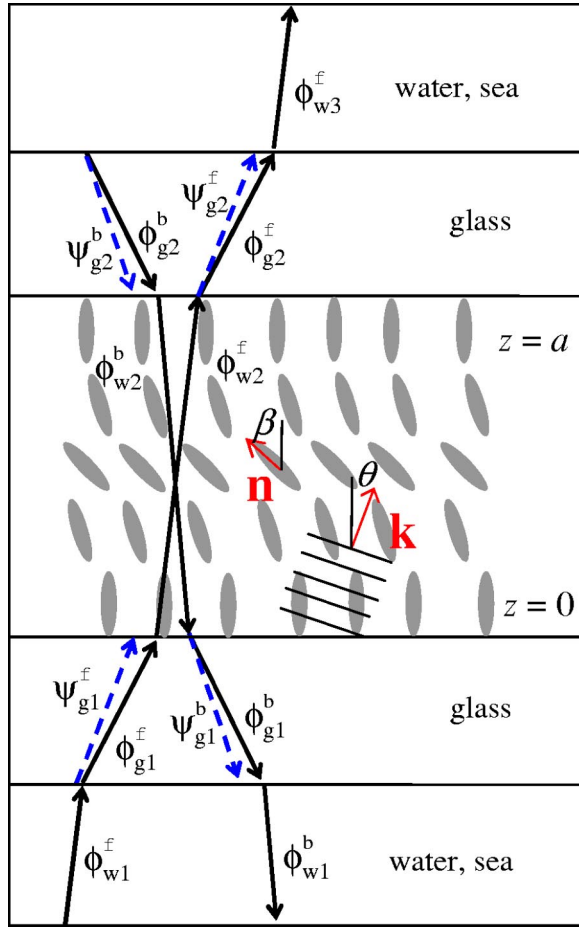


FIG. 1. (Color online) Schematic representation of liquid-crystal cell and how sound waves travel through it. The solid lines indicate the longitudinal sound waves which are produced as the original sound wave propagates forward from the bottom/first layer represented with f superscripts and the backward propagating sound waves created by reflection at the interfaces represented with b superscripts. The change in direction of the waves at each layer interface are required by Snell's law. In the solid glass layers, the dashed lines represent the transverse sound waves. There is only one in each direction for isotropic solids such as glass.

$$\phi_n^m = A_n^m e^{i(\pm k_n^l z \cos \theta_n^l + k_n^l x \sin \theta_n^l - \omega t)}, \quad (2.1)$$

where m is f to represent the forward-traveling wave with $k_n^l z$ or is b to represent the backward-traveling wave with $-k_n^l z$, and n is $w_i; i=1,2,3$ to indicate one of the liquid layers or $g_j; j=1,2$ to indicate one of the solid (glass) layers. The z axis direction is normal to the glass surface. The forward-traveling wave, $A_{w_1}^f$, in the first liquid layer is a known input. Also in the last liquid layer, only the forward-traveling wave, $A_{w_3}^f$, may have a nonzero value, $A_{w_3}^b = 0$. In the glass because it is an isotropic solid, two plane transverse waves are also present

$$\psi_n^m = B_n^m e^{i(\pm k_n^l z \cos \theta_n^l + k_n^l x \sin \theta_n^l - \omega t)}. \quad (2.2)$$

The waves present in each layer are related to each other because certain conditions must be met at the boundaries between layers. There are four boundaries between layers in the system, two between water and glass and two between liquid crystal and glass. Snell's law must be obeyed and three other conditions must be met at each boundary: the component of the displacement normal to the boundary must be continuous, the tangential stress component in the glass must be zero assuming that the fluids are nonviscous, and the normal stress of the solid layer must equal the over pressure in the fluid layer [14]. Assuming plane waves, those three boundary conditions can be written as

$$(\phi_{w_i}^f - \phi_{w_i}^b) k_{w_i}^l \cos \theta_{w_i}^l = (\phi_{g_j}^f - \phi_{g_j}^b) k_{g_j}^l \cos \theta_{g_j}^l - (\psi_{g_j}^f + \psi_{g_j}^b) k_{g_j}^l \sin \theta_{g_j}^l, \quad (2.3)$$

$$(\phi_{g_j}^f - \phi_{g_j}^b) (k_{g_j}^l)^2 \sin 2\theta_{g_j}^l + (\psi_{g_j}^f + \psi_{g_j}^b) (k_{g_j}^l)^2 \cos 2\theta_{g_j}^l = 0, \quad (2.4)$$

$$\rho_{w_i} (\phi_{w_i}^f + \phi_{w_i}^b) = \rho_{g_j} ((\phi_{g_j}^f + \phi_{g_j}^b) \cos 2\theta_{g_j}^l - (\psi_{g_j}^f - \psi_{g_j}^b) \sin 2\theta_{g_j}^l), \quad (2.5)$$

evaluated with $t=0$, $x=0$, and $z=z_{i,j}$ the location of the boundary for $\{i,j\} = \{1,1\}, \{2,1\}, \{2,2\}, \{3,2\}$. These 12 equations are solved simultaneously for the 12 unknown amplitudes.

The coupling of the acoustic wave and the local director of the liquid crystal is derived from continuum elastic theory [12]. Considering thermodynamics the configuration of the liquid crystals can be determined for different sound intensities by energy minimization. This requires contributions to the energy from the sound interaction, the liquid-crystal elastic interaction, and the wall boundary liquid-crystal interaction. The same assumptions made in previous work regarding the form of these contributions were used again. In previous work, the acoustic wave liquid crystal interaction energy was derived to be

$$\langle V_{int} \rangle = \frac{1}{2} u_2 (\Delta \rho)^2 (\vec{k} \cdot \vec{n})^2. \quad (2.6)$$

The wall boundary liquid-crystal interaction was assumed to be the infinite anchoring energy case in which the first layer of liquid-crystal molecules in contact with the wall have a fixed orientation. The derivation to determine the optimum director profile via a free energy minimization follows the same reasoning presented in the previous paper; however, the results differ as both forward- and backward-traveling acoustic waves are present in the liquid crystal rather than a single forward-traveling wave. So the interaction energy is

$$\langle V_{int} \rangle = \frac{1}{2} u_2 k_{w_2}^2 [|A_{w_2}^f|^2 \cos^2(\beta - \theta_3) + |A_{w_2}^b|^2 \cos^2(\beta + \theta_3)], \quad (2.7)$$

which is dependent on two of the acoustic wave amplitudes that are determined by the acoustic calculation above. The free energy per unit area can be written as

$$F = \int_0^a dz \left[\frac{1}{2} (K_1 \sin^2 \beta + K_3 \cos^2 \beta) \left(\frac{d\beta}{dz} \right)^2 + \langle V_{int} \rangle \right]. \quad (2.8)$$

A general expression for $\beta(z)$, which satisfies the boundary conditions $\beta(0) = \beta(a) = \beta_0$, can be written as the Fourier series plus a constant

$$\beta(z) = \beta_0 + \sum_{j=1}^{\infty} \beta_j \sin \frac{j\pi z}{a}. \quad (2.9)$$

This differs from the previous work which only considered the specific case of $\beta_0 = 0$. We consider only the leading term β_1 in the Fourier series. Combining Eqs. (2.7)–(2.9) and integrating gives

$$\begin{aligned} F = & \frac{K_3 \pi^2 \beta_1^2}{4a} + \frac{ak_{w_2}^2 u_2}{4} [|A_{w_2}^f|^2 + |A_{w_2}^b|^2 \\ & + \mathbf{J}_0(2\beta_1) (|A_{w_2}^f|^2 \cos(2\beta_0 - 2\theta_{w_2}) + |A_{w_2}^b|^2 \cos(2\beta_0 \\ & + 2\theta_{w_2})) - \mathbf{H}_0(2\beta_1) (|A_{w_2}^f|^2 \sin(2\beta_0 - 2\theta_{w_2}) \\ & + |A_{w_2}^b|^2 \sin(2\beta_0 + 2\theta_{w_2}))], \end{aligned} \quad (2.10)$$

where \mathbf{J}_0 is the Bessel function and \mathbf{H}_0 is the Struve function. This free energy can be expanded in powers of β_1 and then minimized with respect to β_1 . We retain the first three terms of the power expansion to improve the solutions. This gives a value for β_1 .

The final aspect to consider is the transmission of light through the cell. As was noted in the previous paper the important quantity is the effective birefringence which gives the phase retardation of light passing through the liquid crystal. Approximated, in the previous work, for viewing normal to the surface this was written as

$$\Delta n_{eff}[\beta(z)] \approx \Delta n \sin^2 \beta(z). \quad (2.11)$$

Now it is desirable to be able to consider viewing angles that are not normal to the glass surface. So this equation is rewritten to incorporate viewing angle dependence as

$$\Delta n_{eff}[\beta(z)] \approx \Delta n \sin^2 (\{[\gamma_x + \beta(z)]^2 + \gamma_y^2\}^{1/2}), \quad (2.12)$$

where γ_x and γ_y are the components of small viewing angle in the x and y directions, respectively. We initially considered the case in which only changes in the angle in the x direction were allowed. We integrate the effective birefringence over z assuming $\beta(z)$ and γ_x are small with $\gamma_y = 0$,

$$\delta = \frac{2\pi}{\lambda} \int_0^a \Delta n \sin^2 [\gamma_x + \beta(z)], \quad (2.13)$$

$$\begin{aligned} \delta = & \frac{a\pi\Delta n}{\lambda} \{ \pi\beta_1^2 \cos[2(\beta_0 + \gamma_x)] + 4\beta_1 \sin[2(\beta_0 + \gamma_x)] \\ & + 2\pi \sin^2[\beta_0 + \gamma_x] \}. \end{aligned} \quad (2.14)$$

For the last aspect considered in the results section, variations in both the x and y directions need to be allowed. In this case integration of the effective birefringence yields

$$\delta = \frac{2\pi}{\lambda} \int_0^a \Delta n \sin^2 (\{[\gamma_x + \beta(z)]^2 + \gamma_y^2\}^{1/2}), \quad (2.15)$$

$$\delta = \frac{a\pi\Delta n}{\lambda} \{ \pi\beta_1^2 + 8\beta_1(\gamma_x + \beta_0) + 2\pi[(\gamma_x + \beta_0)^2 + \gamma_y^2] \}, \quad (2.16)$$

which is only used in cases where the viewing angle is varied in both the x and y direction.

The optical intensity transmitted through crossed polarizers can be calculated from

$$I_{opt} = I_{min} + I_0 \sin^2 \left(\frac{\delta}{2} \right). \quad (2.17)$$

These equations describe the entire experimental system. We expect any differences between theory and experiment to arise from approximations made in the theory to simplify the calculations, such as ignoring sound attenuation.

III. RESULTS

The theory will be compared to experimental results already published for cells containing 5CB which range in thickness from 150 to 300 μm [13]. Many of the parameters required in the theory have values that can be obtained from the physical system. The cells are made by sandwiching the liquid crystal between glass plates which are 900 μm thick. The frequency of the sound waves was 3.3 MHz. The experimentally measured birefringence was $\Delta n \approx 0.17$, and the wavelength of the laser light was 0.633 μm . The literature values indicate a range of densities and speeds of sound for glass. We used for the purposes of this calculation a representative density of 2.6 g/cm^3 and a speed of 6000 m/s for the longitudinal waves and 3731 m/s for the transverse waves. The speed of sound in the water and liquid crystal was assumed to be 1500 m/s. The Frank's constant K_3 was chosen to have a value in the order of magnitude typically found in liquid crystals, 10^{-6} dyn. The experimental setup briefly has a liquid-crystal cell which can rotate with respect to an optical laser system and an acoustic transducer placed a sufficient distance from the liquid-crystal cell so that the acoustic field is fully formed. The transducer can also be rotated with respect to the orientation of the optical system. This effectively allows one to consider variations in the viewing angle and variations in the angle at which the sound waves meet the surface of the liquid-crystal cell.

Most of the physical parameters of the theory are fixed once a particular material and setup are chosen. One parameter, u_2 , which represents the coupling between the director and the density gradient, at present cannot be calculated and must be computed by fitting the experimental data. In Fig. 2, experimental data for a 290 μm cell with incoming acoustic sound at -17.5° off normal is plotted along with the results from the original and the current theory. The original theory

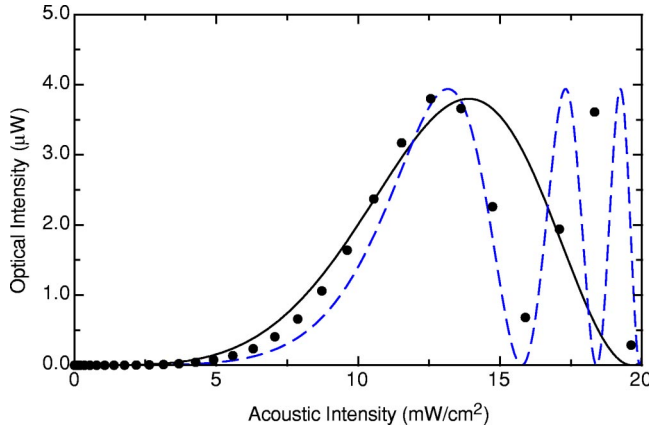


FIG. 2. (Color online) Optical intensity (μW) vs acoustic intensity (mW/cm^2) for a $290\ \mu\text{m}$ thick liquid-crystal cell with sound hitting cell at -17.5° . The symbols are experimental results [13], the solid lines are results from the previous theory [12] and the dashed line is from the current theory.

agrees with the experimental data before the first maximum but departs rapidly after that. The fit of the original theory was only on experimental data up to this first maximum as it was not possible to obtain a reasonable fit if more data points were included. The revised theory is able to match the overall trend of the experiment past the first peak.

We have initially assumed that the viewing angle γ_x and the molecular pretilt angle β_0 match the experimentally measured values of zero. Because the pretilt and viewing angle can be varied in the theory, it is possible to use one or the other as an additional fitting parameter and see how the fit of the experimental data is affected. The results in Fig. 3 are plots of two fits of the data where in one the pretilt of the molecules was used as a fitting parameter with viewing angle still fixed and in the other the viewing angle was a fitting parameter and the pretilt remained a constant. The fitted

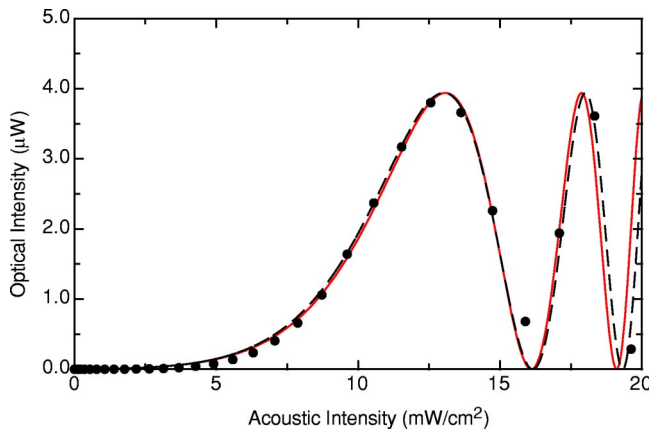


FIG. 3. (Color online) Optical intensity (μW) vs acoustic intensity (mW/cm^2) for a $290\ \mu\text{m}$ thick liquid-crystal cell with sound hitting cell at -17.5° . The symbols are experimental results, the solid lines are results from the current theory using viewing angle γ_x as a fitting parameter (0.56°) and the dashed line is from the current theory using molecular pretilt β_0 at the glass interfaces as a fitting parameter (0.54°).

TABLE I. Fitting parameter u_2 for cells.

Thickness (μm)	$\theta_{acoustic}$ (deg)	u_2 ($\text{cm}^7\ \text{g}^{-1}\ \text{s}^{-2}$)	γ_x (deg)	β_0 (deg)
290	-17.5	1.30×10^3	0.56	0.0
290	-17.5	1.3×10^3	0.0	0.54
294	-19.0	2.51×10^3	-0.40	0.0
295	-18.0	1.64×10^3	0.13	0.0
258	-17.75	4.30×10^3	0.25	0.0

angles in either case are \approx half a degree which is within the uncertainty of the experimental values. This data shows that very good agreement can be obtained with the experimental results with less than a degree change in either one angle or the other. The results for varying either angle are indistinguishable from each other at low acoustic intensities for such small angles.

The theory shows that the performance of the system depends on many physical parameters, some geometrical (cell characteristics) and some associated with the materials (liquid-crystal characteristics). Table I shows the fits for a variety of cells filled with 5CB. The obtained fitting parameters agree with each other fairly well. Since the material remains the same, purely geometrical considerations should account for the differences in the cells' performances and this is confirmed for the theory. Reproducing the exact physical construction of cells for different cells is difficult so to better judge between the performance of different materials comparing the required u_2 for the theory to fit different experimental materials will remove the geometrical considerations.

Apart from the dependence on acoustic intensity, we must also consider the dependence on the angle of the incoming sound wave. The experiments show multiple peaks in the response of the liquid crystal to acoustic intensity as the angle of the incoming sound wave varies. Some of these peaks are quite narrow. This can be understood because in systems with more than two layers reflected waves are possible which allows for the possibility of resonance effects. Depending on materials and geometry of the system nearly all the sound may be transmitted through at different angles. In addition, sound can travel simultaneously as a longitudinal wave and a transverse wave in solids. This means that a non-negligible sound intensity may be present at angles larger than the critical angle for the longitudinal sound waves. Indeed for experiments on a liquid-crystal cell that is $300\ \mu\text{m}$ thick the best response is seen at an angle of -17.5° .

In Fig. 4, the optical response observed for a fixed acoustic intensity is plotted versus the angle of the sound wave for both experimental results and predictions of the theory. The two parameters, u_2 and β_0 , used in the theory are based on a fit of the experimental data for a $290\ \mu\text{m}$ cell of 5CB at its optimum angle of -17.5° . Note that there is no further fit to the angular dependence. The theory predicts the best response in the same angle range as the experiment and also predicts that the peak will have a narrow shape. In addition both theory and experiment show a broader weaker peak around 8° – 10° . The theory has an additional peak predicted at 12.5° that is absent in the experimental data. In Fig. 5,

results are shown for a cell that is $150\ \mu\text{m}$ thick. In this case the sharp peak has shifted to a lower angle in the experimental data and the broad peak at lower angle has become so much weaker that it is barely distinguishable from the dark state. The theory also predicts that the peak shifts to lower angles and that the broader peak at lower angles is much weaker. The shifted peak in the theory has also become much sharper than the experimental result. Overall the theory predicts the behavior as the sound angle changes as well as how these changes depend on thickness. The peak at 12.5° present in the theory for the thicker cell is also present at this cell thickness. The extra peak in the theory represents a resonance condition which is dependent on the dimensions and geometry of the cell present in the theory that is not met in the real experimental system. This is possible as the theory assumes infinite dimensions for the size of the cell while the real system has finite boundaries.

In addition to the dependence of optimal acoustic angle on thickness, the optical response to a low acoustic intensity also depends on the liquid-crystal thickness in the cell. The original theory predicted that the optical phase retardation scales as a^5 , where a is the liquid-crystal thickness in the cell, provided that the acoustic angle is held constant. In our current theory, which considers acoustic transmission and reflection in detail, we see that the thickness dependence may be more complex for two reasons. First, changing the thickness changes the acoustic resonance conditions, which changes the acoustic intensity in the liquid crystal. Second, as we have already seen, changing the thickness changes the optimal acoustic angle. The experimental measurements were not made at a constant acoustic angle, but at the optimal angle for each cell thickness.

To see this more clearly for a given set of fitting parameters the optical intensity at a sound intensity of $1\ \text{mW}/\text{cm}^2$ was tracked as a function of both the angle of the incoming acoustic wave and the thickness of the liquid crystal. In Fig. 6, the results are shown as a density plot as a function of acoustic angle and cell thickness. The grayscale color change from white to black corresponds to increasing optical intensities. The plot shows that certain acoustic angles are optimal

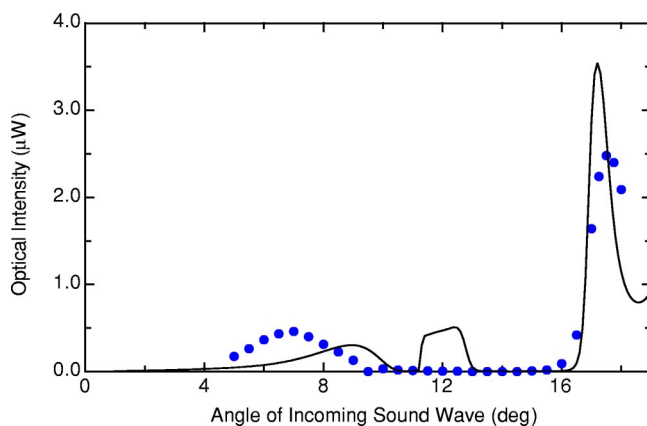


FIG. 4. (Color online) Optical intensity (μW) vs angle of incoming sound wave for a $290\ \mu\text{m}$ thick liquid-crystal cell. The symbols are experimental results, and the solid line is the result from the current theory.

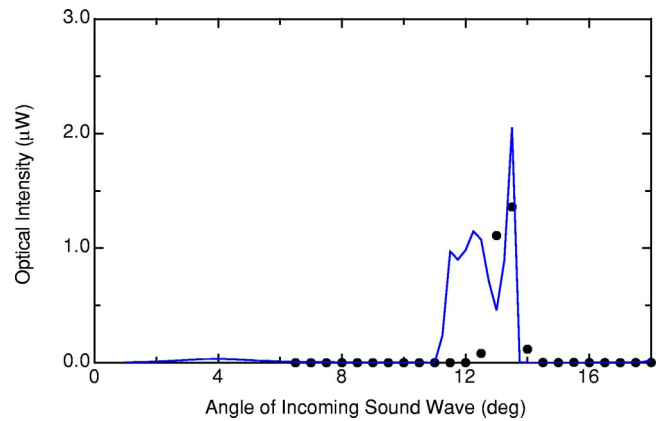


FIG. 5. (Color online) Optical intensity (μW) vs angle of incoming sound wave for a $150\ \mu\text{m}$ thick liquid-crystal cell. The symbols are experimental results, and the solid line is the result from the current theory.

and these angles change gradually as the cell thickness changes. Similar trends are seen at a higher acoustic intensity of $2\ \text{mW}/\text{cm}^2$ in Fig. 7. The regions that had the greatest response at the lower intensity have had the largest increases in their intensity. This follows from the shape the theory predicts at a particular thickness and acoustic angle as seen in Fig. 3. It is difficult to analytically extract the thickness dependence of the acoustics problem as the solution of the 12 equation system has many terms present. The dependence on thickness predicted by the current theory is consistent with the experimental measurements [13] even though it is not exactly a^5 .

The optical response observed is dependent on the view-

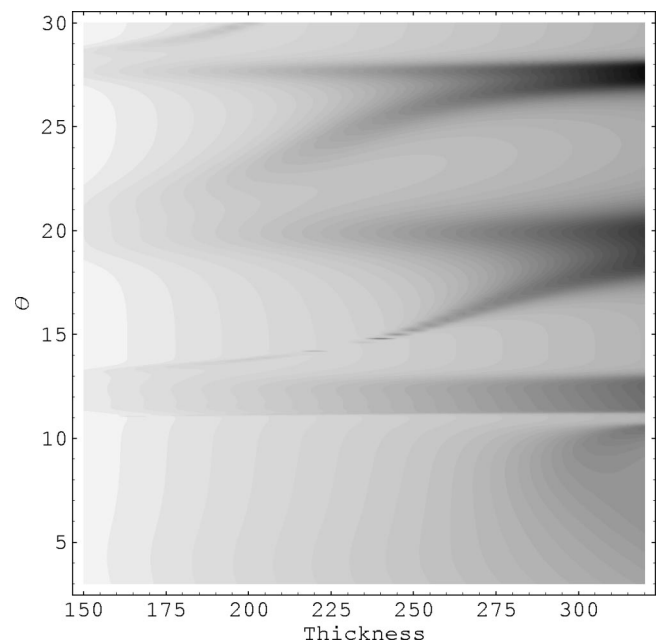


FIG. 6. The optical intensity is denoted by grayscale color as a function of angle of incoming sound wave (deg) and cell thickness (μm). Grayscale color changes from white to black denotes increasing intensity. The incoming sound wave has an intensity of $1\ \text{mW}/\text{cm}^2$.

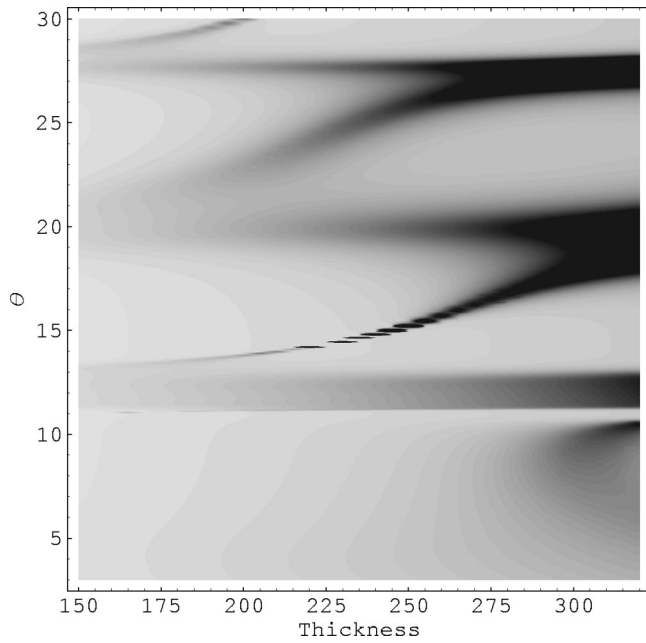


FIG. 7. The optical intensity is denoted by grayscale color as a function of angle of incoming sound wave (deg) and cell thickness (μm). Grayscale color from white to black denotes increasing intensity. The incoming sound wave has an intensity of 2 mW/cm^2 .

ing angle. In Figs. 8 and 9, the behavior observed in the experimental system and predicted by the theory for the viewing angles from 0° to 4° are shown for the optical response versus acoustic intensity. Note that the location of the first maximum is shifted from higher acoustic intensities to lower values as the viewing angle increases. Also at the larger deviations from normal viewing the optical intensity observed at zero acoustic intensity becomes significant. The amount of shifting per degree of change in viewing angle are similar between the theory and experimental results for the smallest deviations. At the larger deviations the trend is correctly predicted by the theory but the theory shows a slightly

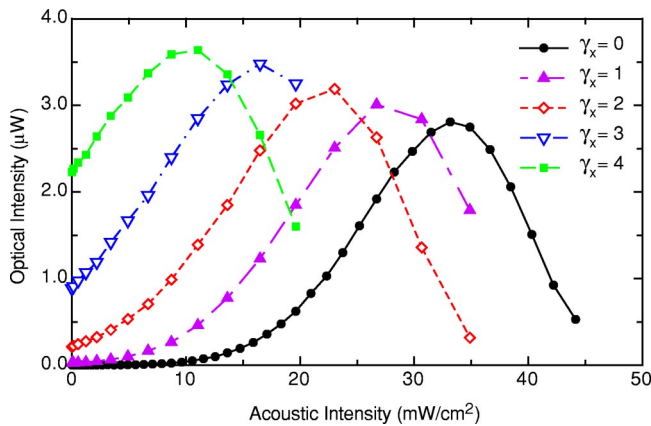


FIG. 8. (Color online) Optical intensity (μW) vs acoustic intensity (mW/cm^2) from experimental data for a $290 \mu\text{m}$ thick liquid-crystal cell with sound hitting the cell at -12.5° . The viewing angle is varied 0 (black, —), 1 (purple, - - -), 2 (red, - · -), 3 (blue, — · —), 4 (green, — —).

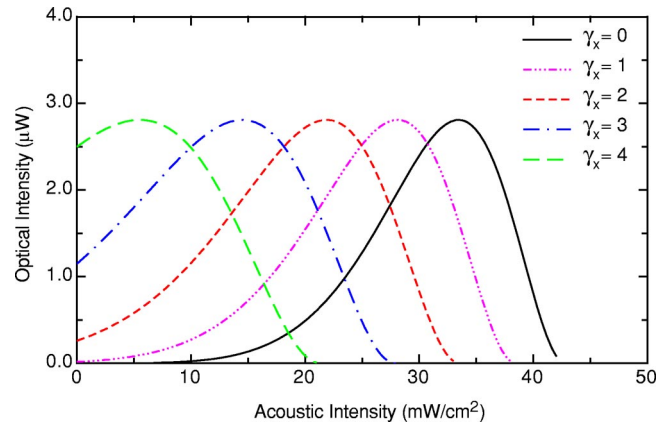


FIG. 9. (Color online) Optical intensity (μW) vs acoustic intensity (mW/cm^2) from theory for a $290 \mu\text{m}$ thick liquid-crystal cell with sound hitting the cell at -12.5° . The viewing angle is varied 0 (black, —), 1 (purple, \cdots —), 2 (red, - · -), 3 (blue, — · —), 4 (green, — —).

larger shift than that seen in the experiment. The experimental results also show a dependence of the maximum optical intensity observed as the viewing angle varies. The theory as derived does not predict such a trend.

The theory has given good agreement with the experimental results, and we now want to turn our attention to conditions not yet seen in the experimental system. This is one practical value of the theory in that new cases can quickly be evaluated, and the best cases can be selected for experimental study. From considerations of the original theory having the liquid crystals oriented at 45° to the incoming sound wave is a potentially more responsive condition. So in Fig. 10, we consider a cell that has a molecular pretilt of 45° and the sound being transmitted normal to the glass surface viewed at 45° and 44.5° compared to results for a system with no molecular pretilt (homeotropic) but the sound trans-

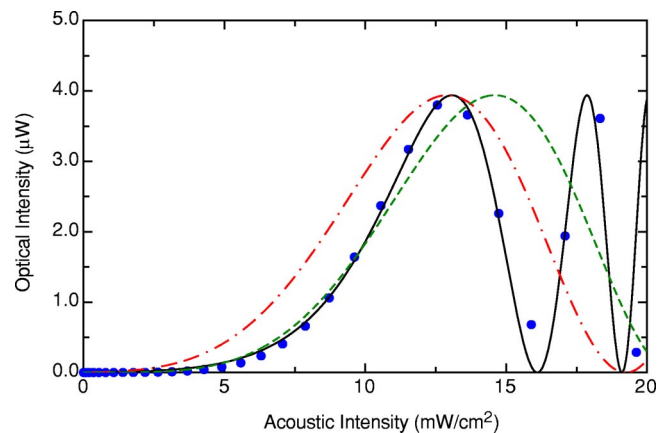


FIG. 10. (Color online) Optical intensity (μW) vs acoustic intensity (mW/cm^2) for a $290 \mu\text{m}$ thick liquid-crystal cell. The solid (black) line is for the theory with no molecular pretilt, 0.56° viewing, and sound hitting the cell at -17.5° . The dashed (green) line is for the theory with 45° molecular pretilt, 45° viewing, and sound hitting normal to the cell surface. The dot-dash (red) line is for the theory with 45° molecular pretilt, 44.44° viewing, and sound hitting normal to the cell surface.

mitted at 17.5° viewed at 0.56° . With no sound transmission a cell with no pretilt and some specified pretilt do not have the same response at a given viewing angle; however, the behaviors can be mapped onto each other. When the molecular pretilt is increased to 45° , the viewing angle that corresponds to normal viewing for a system with no pretilt shifts to $\approx 45^\circ$. The benefit of a pretilt is that the acoustic resonance conditions are not affected for changes in pretilt and a different pretilt may allow a resonance condition to be exploited. The overall shape of the curve has changed although the value of the acoustic intensity at the first maxima in optical intensity has not changed significantly. The broader shape of the curve with molecular pretilt shows that the system is sensitive over a large range of acoustic intensities. This is a desired property for a real device. So the new case could be considered the better of the two, based not on which requires the smallest acoustic intensity to reach its maximum optical response but on this other requirement for applications. The small change in viewing angle from 45° to 44.44° shows how sensitive the system remains to viewing angle. Consideration of this case emphasizes that there are several important factors guiding the optimization of parameters for a real application.

For a real portable device, the acoustic intensity required to reach an optical peak is one useful criterion in ranking the performance of cases. Another criterion is that the system shows roughly equal sensitivity at all sound intensities up to the sound intensity when the optical response first reaches its maximum value. This means that variations of sound intensities will have an easily interpretable meaning when viewed. The first criterion is dependent on the thickness of the liquid-crystal cell and viewing angle or molecular pretilt. In addition it is dependent on the coupling constant, u_2 , which depends on the material. From the predictions of the theory, any material could be made to give a desired level of response by simply making the cell thicker. In practice the maximum possible thickness is limited by the difficulty of achieving good alignment in thick cells. The cell alignment is critical for giving a good dark state and large intensity range. In addition other desirable properties such as the speed of response, not covered in this theory, degrade with increasing thickness. So for the real system an optimal thickness that has the best tradeoff of response versus speed will have to be chosen. The second criterion can be manipulated regardless of the material via changes in the geometrical parameters of the cell and its orientation with respect to the sound waves. However, it is also dependent on the viewing angle. In a real device visual information from different regions of a two-dimensional image is viewed by the eye or a camera at different angles. This angle dependence is difficult to remove in practice. This viewing angle dependence means that for a real device having the optimal performance at one viewing angle may not be important as having acceptable performance over a wider range of viewing angles. Indeed, the strong viewing angle dependence might lead one to question whether a usable device is even possible. Thus, it is worthwhile to use this theory to explore what the final image from a device may look like.

The process of viewing a real image was modeled using

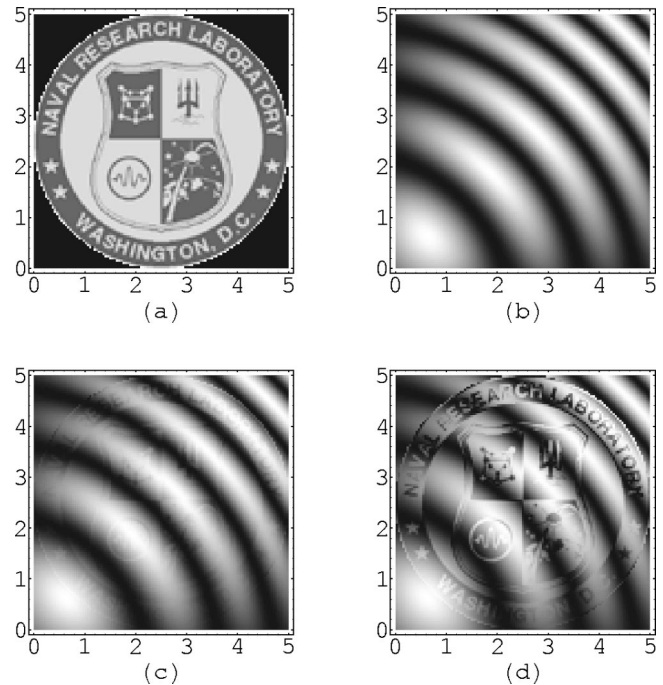


FIG. 11. Incoming sound intensity proportional to brightness of (a) test image. Calculated response of $5 \times 5 \text{ cm}^2$ liquid-crystal cell that is $290 \mu\text{m}$ viewed from 30 cm away (b) for no base sound intensity, (c) for 1.1 mW/cm^2 , and (d) for 5 mW/cm^2 .

the theory developed in this paper. For this calculation, a viewing plate $5 \times 5 \text{ cm}$ was subdivided into 115×115 equal sized pixels. The individual regions of the liquid crystal were assumed to reorient independent of each other. The sound intensity that reaches a particular liquid-crystal pixel was proportional to the gray scale intensity of the sample image in Fig. 11(a). A white pixel corresponds to full sound intensity and black to no sound intensity. The monocular viewer (eye or camera) is 30 cm distant from the liquid-crystal cell and at a location such that the lower left corner of the image is being viewed at 2° from the normal in both directions. This was chosen so that the cross pattern produced by linear cross polarizers would not obstruct the view produced by the sound waves. The viewing angle for each pixel can now be computed from the geometry and used in the solution of the theory in each pixel. Figure 11 shows the results for a few different sound intensities. Figure 11(b) shows that without any sound intensity reaching the liquid crystal a pattern of bright and dark fringes would be seen. As the sound intensity increases the image appears superimposed on the fringes. It is first visible at about $1-1.1 \text{ mW/cm}^2$, Fig. 11(c) shows the value at 1.1 mW/cm^2 and is easily identified at 5 mW/cm^2 in Fig. 11(d). The most sensitive parts of the image are the regions that were between the brightest and darkest strips of Fig. 11(a). Some parts of the image are not viewable, but clearly sufficient information is present to discern the image.

IV. DISCUSSION

We have considered improvements to a promising continuum theory to model the coupling of acoustic waves with

liquid-crystal behavior. The previous work for the original theory confirmed the important influence choice of material has on the performance and response of liquid crystals to ultrasonic waves. There were however several features of recent experimental results that the original theory could not predict. We incorporated more details of the acoustics of the physical system which resulted in a theory that predicts all of the trends observed in the experimental system. The theory makes a prediction of the optical intensity versus acoustic intensity that is consistent with experimental results. The presence of optimal (resonant) acoustic angles for the liquid-crystal cell is confirmed in the theory and its predictions compare favorably with the experiments. The change in the optimal acoustic angle as liquid-crystal thickness varies is also correctly captured.

The results considered in the current paper have focused on variations in geometrical considerations of cell construction and orientation of the cell. These results demonstrate the importance of choosing the appropriate cell geometry as well as the best material to provide the best response for practical applications. As the theory is so consistent with the experi-

mental results it now provides a tool to rapidly consider further alterations to the physical geometry to alter the performance of the liquid-crystal cell. Finally, we have considered in the theory how the strong angle dependence of the liquid-crystal cell impacts on their usability for real applications. Using dimensions that might be seen in a real device the theory predicts bright and dark fringes that mask parts of a real image. The spacing between the fringes is sufficient to allow enough of the image to show that it can be discerned. It should be possible to further improve these results by post processing of the image or small changes in the viewing angle so that every region of the cell is periodically viewed at an optimal angle.

ACKNOWLEDGMENTS

This work was supported by the Office of Naval Research and the Naval Research Laboratory. A.P. Malanoski and V. A. Greayna were supported by the National Research Council.

-
- [1] S. Candau and S.V. Letcher, in *Advances in Liquid Crystals*, edited by G.H. Brown (Academic, New York, 1978), p. 167.
 - [2] O.A. Kapustino, in *Physical Properties of Liquid Crystals*, edited by D. Demus, J.W. Goody, G.W. Gray, and H. Spiess (VCH, Wiley, New York, 1999).
 - [3] O.A. Kapustino, *Sov. Phys. Acoust.* **20**, 1 (1974).
 - [4] J.-L. Dion, *C. R. Seances Acad. Sci., Ser. B* **284**, 219 (1977).
 - [5] J.-L. Dion and A.D. Jacob, *Appl. Phys. Lett.* **31**, 490 (1977).
 - [6] J.-L. Dion, *C. R. Seances Acad. Sci., Ser. B* **286**, 383 (1978).
 - [7] J.-L. Dion, *Appl. Phys. Lett.* **50**, 2965 (1979).
 - [8] J.-L. Dion, R. Simard, A.D. Jacob, and A. Leblanc, *Ultrasonics Symposium* (IEEE, New York, 1979), p. 56.
 - [9] J.S. Sandhu, W.J. Popek, and H. Wang, U.S. Patent No. 5,796,003 (18 August 1998); U. S. Patent No. 6,049,411 (11 April 2000).
 - [10] D.W. Gerdt, M.C. Baruch, and C.M. Adkins, *Proc. SPIE* **3635**, 58 (1999).
 - [11] J.S. Sandhu, H. Wang, and W.J. Popek, *Proc. SPIE* **2955**, 94 (2000).
 - [12] J.V. Selinger, M.S. Spector, V.A. Greanya, B.T. Weslowski, D.K. Shenoy, and R. Shashidhar, *Phys. Rev. E* **66**, 051708 (2002).
 - [13] V.A. Greanya, M.S. Spector, J.V. Selinger, B.T. Weslowski, and R. Shashidhar, *J. Appl. Phys.* **94**, 7571 (2003).
 - [14] H.F. Pollard, *Sound Waves in Solids* (Pion, London, 1977).